PREPRINT

The Seismic Fingerprint of Tree Sway

Josefine Umlauft[1] | Karin Mora[2] | Fabian Limberger[3] | Kilian Gerberding[4] | Christian Wirth[5] | Christiane Werner[6] | Teja Kattenborn[4]

[1]ScaDS.AI - Center for Scalable Data Analytics and Artificial Intelligence, Leipzig University, Saxony, Germany

[2]Institute for Earth System Science & Remote Sensing, Leipzig University, Saxony, Germany

[3]Goethe University Frankfurt am Main, Hessen, Germany

[4]Sensor-based Geoinformatics, Faculty of Environment and Natural Resources, University of Freiburg, Baden-Württemberg, Germany

[5]Institute of Systematic Botany and Functional Biodiversity, Leipzig University, Saxony, Germany

[6]Ecosystem Physiology, Faculty of Environment and Natural Resources, University of Freiburg, Baden-Württemberg, Germany

Correspondence

Josefine Umlauft, ScaDS.AI

Dresden/Leipzig, Leipzig University

Email: josefine.umlauft@uni-leipzig.de

Funding information

1. Climate change is increasing the frequency and intensity of extreme events like heat waves, droughts, and storms, placing forests under growing physiological and mechanical stress.
2. Common indicators of tree stress, such as sap flow, stomatal conductance, water potential, or photosynthetic activity, provide valuable insights but are costly, maintenance-intensive, and difficult to scale for continuous, long-term observation. We propose a novel alternative approach:

tracking tree sway through its seismic ground motion signature, referred to as the tree's seismic fingerprint. These wind-induced sway signals are intrinsically linked to the mechanical properties of leaves, branches, and trunks, which change under environmental stress. Seismometers offer key advantages: they are non-invasive, low-maintenance, and easily scalable for tree monitoring across forest plots.

3. Using observations from ground-based seismometers and trunk-mounted accelerometers at the ECOSENSE site in the Black Forest, we isolated and analysed tree sway signals based on spectral decomposition and vibrational mode tracking. We identified consistent tree-dependent sway frequencies around 0.2 Hz and demonstrated that ground-based sensors can capture sway dynamics without direct attachment. Using machine learning, we further showed that wind speed can be reliably predicted from seismic features, revealing that wind-induced mechanical input is encoded in ground motion.
4. These findings show that seismometers can passively monitor both environmental forcing and tree biomechanical response. As such, seismic sensing offers a power-

ful, scalable tool for forest monitoring - capable of capturing stress symptoms tied to both vitality and structural stability in the face of climate extremes.

KEYWORDS

Biomechanical stress, Climate extremes, Forest monitoring, Machine learning, Seismic sensing, Spectral analysis, Tree sway

NOTE: This manuscript is a non-peer-reviewed preprint currently under review at Methods in Ecology and Evolution (MEE).

1 | INTRODUCTION

Forests worldwide are increasingly affected by climate change, particularly through the rise of extreme weather events such as prolonged droughts, heatwaves, and intense storms. These stressors may occur independently or in close sequence, potentially forming compound events that can severely impact forest ecosystems. Droughts accompanied by heatwaves, often referred to as "hotter droughts," exert severe physiological stress by simultaneously reducing water availability and increasing evaporative demand (Allen et al., 2015; Werner et al., 2025). In parallel, the frequency and intensity of storms, involving high winds, heavy precipitation, and convective gust fronts, are rising in many regions, increasing the risk of mechanical damage. Such disturbances can cause branch breakage, stem snapping, or complete uprooting, especially in trees already weakened by drought-induced loss of turgor or reduced root stability. As a result, trees face both physiological and structural vulnerability, highlighting the need to monitor hydraulic as well as biomechanical responses to external environmental stressors.

Addressing the need for scalable, low-maintenance tree monitoring, we propose a novel, non-invasive method using seismometers — ground-based instruments traditionally employed to record earthquakes (Shearer, 2009) and near-surface environmental processes (Larose et al., 2015). While earlier work has shown that trees can dampen

incoming seismic waves (Colombi et al., 2016; Liu et al., 2019), the reverse is also true: trees driven by wind forces can act as seismic sources, transmitting low-frequency vibrations into the ground. Like wind turbines that generate measurable seismic signals (Limberger et al., 2021; Gassner and Ritter, 2023), swaying trees can be detected by nearby broadband or short-period seismometers (Johnson et al., 2019).

This raises a central question: can ground-based seismic sensors provide a contact-free approach to monitoring tree biomechanics across entire forest plots, capturing meaningful sway signals without attaching instruments to the trees themselves?

Existing methods to assess tree stress often rely on physiological measurements, including sap flow sensors, dendrometers, leaf water potential, and stomatal conductance. These indicators are closely tied to internal plant processes but typically require invasive installation, regular maintenance, and are challenging to deploy at scale. In addition to physiological signals, mechanical responses such as stem sway and branch oscillation offer valuable information about tree structure, water status, and exposure to environmental forces. Accelerometers have been widely used for this purpose, providing direct measurements of sway dynamics, including natural frequencies, damping behaviour, and canopy motion (Brüchert et al., 2003; Spatz and Theckes, 2013; Ciruzzi and Loheide II, 2019). While accelerometers offer detailed insight into tree biomechanics, their installation is labor intensive and often limited to individual trees, making them impractical for large-scale forest monitoring.

Recent studies have used accelerometers to track drought-induced changes in tree mechanical properties (Giachetti et al., 2022), to monitor canopy interception processes during and after storms (Ciruzzi and Loheide II, 2021), and to measure tree sway and structural characteristics (van Emmerik et al., 2017). Moreover, Ghonimy et al. (2025) investigated the damping behaviour of olive trees under trunk shaking by analysing transmitted acceleration and energy components such as elastic and damping power. Grande et al. (2023) applied structural engineering methods to dynamically identify vibration frequencies and damping ratios in cherry trees using accelerometers and finite element models, highlighting their potential in tree health monitoring. Wang et al. (2024) studied vibration transmission in walnut trees by comparing theoretical and measured spatial vibration modes, revealing how vibration propagates through the trunk and branches depending on frequency and damping characteristics. Raleigh et al. (2022) estimated snowpack accumulation on conifer canopies.

These studies underscore the potential of accelerometers in tree biomechanics, yet their deployment often involves climbing and securing sensors to individual trees, limiting their deployment at the landscape scale. This is where seismometers offer a major advantage. Installed in the ground and requiring minimal maintenance, they can passively record tree-induced vibrations from multiple sources simultaneously. In this study, we assess whether such seismic recordings can detect key biomechanical traits, especially the natural sway frequency (or eigenfrequency) of trees, a fundamental vibration mode of the tree–soil system.

This frequency, typically between 0.1 and 5 Hz, reflects the mechanical resonance of the whole tree and depends on tree height, trunk diameter (DBH), wood properties, and crown structure (Brüchert et al., 2003; Jackson et al., 2021). For example, Douglas fir (*Pseudotsuga menziesii*) and Ponderosa pine (*Pinus ponderosa*) tend to sway at higher frequencies (0.2–1.5 Hz) due to their vertical form and conical crowns, while European beech (*Fagus sylvatica*) often shows lower sway frequencies and stronger damping, attributed to broader crowns with greater surface area and mass damping from foliage (Moore and Maguire, 2004; Jackson et al., 2019). These species-specific spectral signatures can potentially be revealed through seismic recordings, offering a biomechanical lens into how different trees respond to wind.

Our main ecological question is whether passive seismic sensing can reveal meaningful differences in tree structure and sway dynamics across species and environmental conditions, and thus serve as a tool to assess vulnerability to external environmental stressors, such as storms or drought.

To address this, we analyse co-located seismic and accelerometer data from six trees under natural wind forcing. We identify dominant vibrational modes and evaluate their stability and variability over time, translating these dynamics into seismic features used to predict wind speed. Wind speed serves as a proxy for mechanical forcing on trees, and and estimating it from passive seismic signals offers a means to quantify tree exposure without relying on direct wind measurements. Our results show that ground-based seismic recordings retain rich information about aboveground sway behaviour - highlighting a new, non-invasive pathway for scalable monitoring of tree mechanical responses in forest ecosystems.

2 | MATERIALS AND METHODS

2.1 | ECOSENSE Site and Dataset

ECOSENSE is an interdisciplinary research project and platform located near Ettenheim, Germany, designed to monitor forest ecosystem functioning across multiple spatial and temporal scales (https://www.ecosense.uni-freiburg.de). The ECOSENSE Forest is a structurally heterogeneous forest located at the foothills of the Black Forest, primarily composed of European Beech (*Fagus sylvatica*) and Douglas fir (*Pseudotsuga menziesii*), with additional presence of Norway spruce (*Picea abies*), pedunculate oak (*Quercus robur*), silver fir (*Abies alba*), and Scots pine (*Pinus sylvestris*), consisting of trees of varying ages and arranged in both mixed and pure patches. The network integrates a diverse suite of in situ and remote sensors that continuously collect comprehensive data from soils, trees, and the atmosphere, spanning from ground level to the forest canopy (Werner et al., 2024). The instrumentation is rapidly expanding and undergoing continuous development to improve measurement capabilities.

In July 2024, the ECOSENSE network was augmented with a set of seismic sensors, installed for long-term quasi-continuous ground vibration monitoring across a mid-sized forest plot of approximately 400 m². Data are recorded at a sampling frequency of 100 Hz (Figure 1A,B). The seismic array comprises six 3-component broadband seismometers (Trillium Compact 120s, Nanometrics) connected to DATA-CUBE³ recorders (Digos, Omnirecs). To optimize seismic coupling and reduce environmental noise, the sensors were buried in 30 cm deep holes resting on concrete slabs (Figure 1C). Complementing the long-term seismometer array, accelerometers (Episensor, Kinemetrics) were temporarily mounted on six trees within the plot. For one selected tree per measurement period, three 3-component accelerometers were attached directly to the trunk using lashing straps, with a vertical spacing of 1 meter between sensors (Figure 1B,D). Each accelerometer was connected to a DATA-CUBE³ recorder. Three trees were equipped and monitored for 6 days in July 2024, and three additional trees for 9 days in August 2024, enabling comparison across species, stem diameters and heights. The instrumented individuals include Douglas fir and beech trees, with diameters at breast height (DBH) ranging from approximately 30 to 60 cm, and heights (H) between about 26 to 36 m (Table 1).

TABLE 1 Overview of instrumented trees with acceleration measurement period, including species identity, diameter at breast height (DBH), tree height (H) and DBH/H² (after Moore and Maguire (2004)). Also shown are median values per tree for: primary peak amplitude (unitless), primary peak frequency (Hz), mean and total power from the power spectral density (PSD) in decibels (dB), and the PSD peak frequency (Hz).

Tree ID	ACC Period	Species	DBH	H	DBH/H²	Primary Amp	Primary Freq	Mean PSD	Total PSD	PSD Peak Freq
4_62	07/2024	Douglas Fir	59.84	35.3	0.048	6,359	0.25	1,298	118,156	0.26
8_18	07/2024	Douglas Fir	30.24	28.0	0.039	2,964	0.23	1,272	115,726	0.24
4_67	07/2024	Beech	39.15	30.5	0.042	18,718	0.23	3,400	309,409	0.23
6_23	08/2024	Beech	40.11	26.4	0.058	38,063	0.20	6,105	555,527	0.19
5_28	08/2024	Beech	38.20	28.6	0.047	74,147	0.20	13,183	1,199,672	0.18
5_64	08/2024	Beech	34.06	27.9	0.044	18,091	0.20	2,960	269,397	0.19

2.2 | Spectral and Eigenvector Analysis

All seismic and acceleration time series were preprocessed by averaging the two horizontal components (north-south and east-west), discarding the vertical component, applying a bandpass filter (0.1–1 Hz), downsampling to 5 Hz, and masking known data gaps to avoid introducing artifacts in spectral estimates.

To captured the dynamic frequency content of tree sway, time-resolved spectrograms were computed using short-time Fourier transforms (STFT) via `scipy.signal.spectrogram`, with window lengths ranging from 10 to 30 minutes depending on sensor type and dataset. Each window was tapered with a Hann function and 50 % overlap to balance temporal and spectral resolution. From each window, we extracted up to three dominant frequency peaks, classified as primary, secondary, and tertiary, using a prominence- and spacing-based peak detection. These peaks were tracked over time to evaluate their persistence and variability.

In parallel, unfiltered power spectral densities (PSDs) were computed from one-minute segments using Welch's method (Welch, 1967) to characterize the long-term frequency distribution of vibrational energy. PSDs were grouped by wind speed bins and averaged to reveal wind-dependent spectral behaviour. To reduce the influence of extreme outliers, the top 25 % of PSDs by amplitude were excluded. Together, the spectrogram-based peak and PSD evolution enabled systematic comparisons across tree species, biomechanical traits (H, DBH, DBH/H²), and sensor configurations. To analyse coherent motion patterns, we applied singular value decomposition (SVD) using `numpy.linalg.svd` to the spectrograms of individual sensor time series. Each decomposition yielded spatial and temporal eigenvectors that isolate dominant vibrational modes specific to a given sensor.

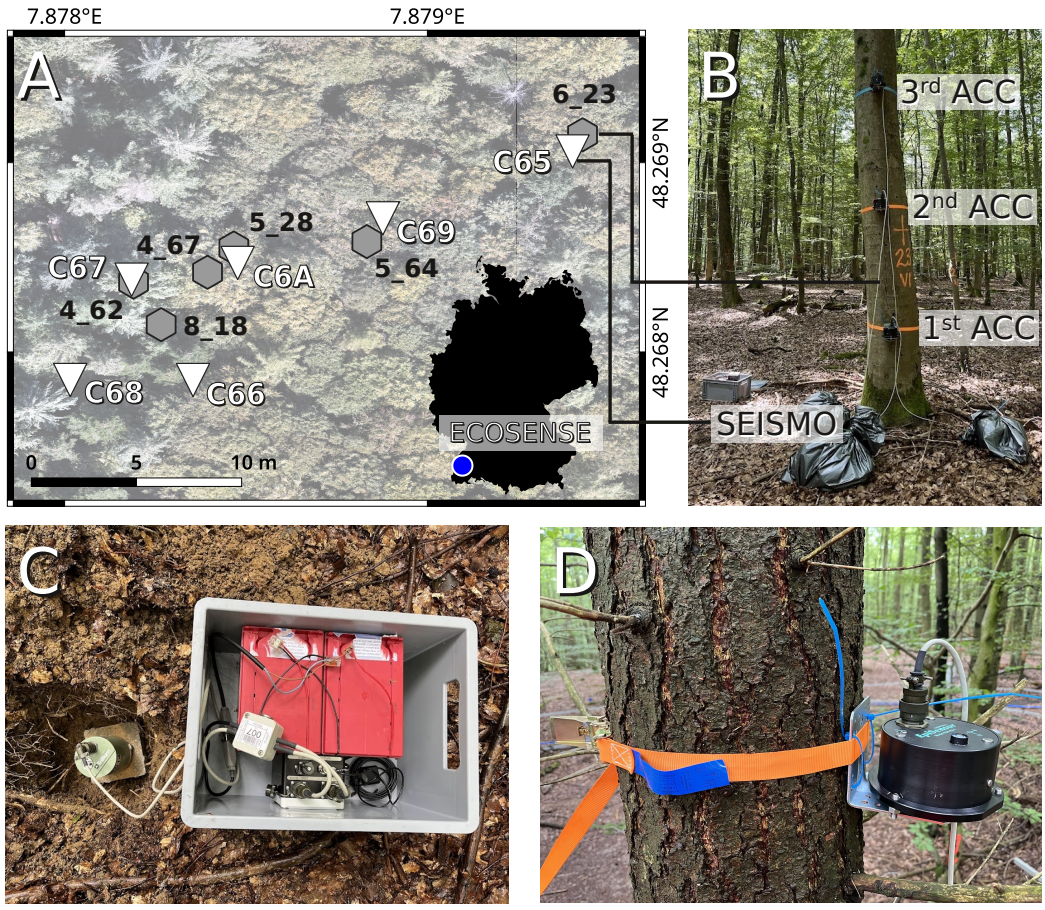

FIGURE 1 **A** Seismic instrument set-up at the ECOSENSE site within the Black Forest. The locations of the belowground seismometers are indicated by white triangles, the locations of trees/trunks equipped with three vertically aligned accelerometers are indicated by grey hexagons. **B** Picture of the field deployment of an instrumented tree with three trunk-mounted accelerometers (ACC) and one co-located seismometer (SEISMO). **C** The seismometer: A Trillium Compact 120 s sensor (Nanometrics) was buried at 30 cm depth, based on a concrete slab and connected to a DATA-CUBE³ (Digos, Omnirecs) recorder, a GPS antenna and batteries (9 V, 130 Ah, Patura), all stored in a grey box. **D** Exemplary accelerometer: Three Episensors (Kinemetrics) were strapped to the trunk with a vertical spacing of 1 m connected to a DATA-CUBE³ (Digos, Omnirecs) recorder, a GPS antenna and batteries (9 V, 130 Ah, Patura) as well.

Although we refer to this framework as SVD, it is mathematically equivalent to principal component analysis (PCA) when applied to mean-centered data, with the right singular vectors corresponding to principal components and the singular values relating to explained variance. By comparing the resulting eigenvectors across co-located instruments (one ground-based seismometer and three accelerometers mounted at different heights on the same tree), we charac-

terized differences in vibrational behaviour and sensitivity. This Fourier- and eigenvector-based framework enables robust identification of key sway dynamics across sensor types and tree structures under varying environmental conditions.

2.3 | Gradient-boosted decision tree model

We trained gradient-boosted decision tree models using the XGBoost framework (Chen and Guestrin, 2016) to predict wind speed from seismic features. The input features consisted of the median, across all seismometers, computed at 10-minute time steps. Spectral features included the primary, secondary, and tertiary peak frequencies and their corresponding amplitudes extracted from the spectrograms as well as the seismic power within the 0.1–1 Hz frequency band. In addition, we incorporated summary statistics derived from power spectral density (PSD) vectors, including total PSD power, mean PSD power, and peak PSD frequency between 0.1 and 1 Hz. These PSD-based features provided complementary descriptors of spectral energy distribution and enhanced the feature space beyond individual peaks. Prior to modeling, all features were smoothed using a rolling mean filter to reduce high-frequency noise and improve signal stability.

To guide the choice of model validation strategy and ensure independence between training and test samples, we assessed the temporal autocorrelation structure of all input features and the wind speed target. This step was necessary to avoid data leakage from temporally correlated observations, which can otherwise lead to overestimated model performance. We computed autocorrelation functions for each feature, using normalized time series derived from the median across all seismometers (see Supporting Figure S3). Features such as seismic power and spectral peak amplitudes showed relatively slow autocorrelation decay, while higher-order spectral peaks decayed more rapidly. Most features reached minimal autocorrelation around a 7-day lag, which informed our choice of block size for cross-validation. A block-wise train-test split with a 7-day window was therefore implemented to minimize overlap between temporally dependent samples.

Model training, preprocessing, and evaluation were performed using the Python libraries XGBoost, scikit-learn, and SHAP. Model performance was evaluated using stratified 5-fold cross-validation with preserved block structure.

For model interpretability, SHapley Additive exPlanations (SHAP) analysis (Lundberg and Lee, 2017) quantified the marginal contribution of each feature to the predictions. This combined approach of autocorrelation-aware splitting, cross-validation, and SHAP interpretation provided robust and transparent insights into the seismic indicators of wind speed.

3 | RESULTS

3.1 | Spectral responses to wind loading

To capture both the time-varying and broadband aspects of wind-driven sway and to reveal how structural and environmental factors modulate tree vibrational behaviour, we used a combined approach of spectrogram-based peak and PSD evolution. The synchronized recordings from accelerometers and a co-located seismometer revealed a consistent vibrational signature of tree sway dynamics. During the monitoring period from July 5–10, 2024, all sensors - whether trunk-mounted accelerometers or buried seismometer (see Figure 2A for instrument set up) - captured a persistent energy concentration around 0.25 Hz, as shown in the time-frequency spectrograms (Figure 2B). This dominant sway frequency was most evident during windier intervals and remained stable throughout the observation window. Spectral peak tracking using 10-minute moving windows showed that the primary frequency component (highlighted in red) persisted near 0.25 Hz, while secondary and tertiary peaks (blue and grey, respectively) appeared more intermittently (Figure 2C). When comparing amplitude spectra across all sensors, a vertical gradient in sway intensity was observed, with higher-amplitude responses recorded by accelerometers mounted higher on the trunk and ground-based seismometers exhibiting lower sensitivity at higher frequencies (Figure 2D).

Wind-dependent PSDs derived from sensors at tree *4_62* (Douglas fir) exhibit a distinct frequency peak at 0.25 Hz that increases significantly with wind speed (Figure 3). The centre frequency of this peak is consistently observed both in trunk acceleration and in seismic ground motion. A slight increase in seismic noise level between 0.16 and 0.6 Hz, even during very low wind speeds of <2 m/s, corresponds to ocean-generated microseismic noise (Hasselmann (1963), Figure 3A). Nevertheless, superimposed on this background noise is the tree's fundamental vibration, which

becomes more pronounced during strong wind conditions. In contrast to PSDs derived from trunk accelerometers, the seismic fundamental frequency is not discernible during wind speeds of 0-1 m/s, even though the trunk sways slightly. An additional distinct peak at 1.15 Hz, observed across all seismic sensors but not detected by the accelerometer, correlates with wind speed and is attributed to nearby wind turbines located approximately 3 km from the study site. This phenomenon will be explained in the discussion.

Time-resolved analysis of spectral features revealed consistent patterns across time, sensors and tree species and their individual biomechanical traits. In the frequency domain (see Supporting Figure S1), primary, secondary, and tertiary peaks displayed clear clustering by species, particularly for Douglas Fir and Beech individuals, with relatively stable yet distinct spectral bands. Over time, minor shifts in frequency content appeared to co-occur with windier conditions, particularly for tertiary peaks, which were more variable in accelerometer data. The amplitude evolution (see Supporting Figure S2) showed pronounced peaks aligned with increased wind speed, especially in primary components. Seismometers typically recorded sustained, low-frequency, high-amplitude motion, while accelerometers captured more transient, high-frequency bursts during periods of elevated wind activity. In the PSD-based metrics (Figure 4), total and mean power increased during wind events across most species. The PSD peak frequency followed similar temporal dynamics to the frequency-based peaks and showed higher variance in accelerometer recordings. Together, these observations confirm consistent feature evolution across all three spectral descriptors under changing wind conditions.

Distributions of peak vibrational features, summarized across all time windows and grouped by species (Figure 5, Table 1), revealed clear species-specific patterns. Primary peaks tended to be the strongest and most tightly clustered, while secondary and tertiary peaks showed greater spread and lower median amplitudes. Beech trees exhibited substantially higher primary peak amplitudes (18,091–74,147) and total PSD power (269,397–1,199,672 dB) than Douglas firs (amplitudes: 2,964–6,359; total PSD: 115,726–118,156 dB), whose signals were characterized by slightly higher primary (0.23–0.25 Hz) and PSD peak frequencies (0.24–0.26 Hz) compared to beech (both 0.18–0.23 Hz). These trends were consistent across trees with varying diameters at breast height (DBH) within each species. Median values and violin plot shapes further showed that beech signals often had broader or more asymmetric distributions, especially for secondary and tertiary peaks. The strongest amplitudes and power values were recorded in August

2024, although the overlap with species identity (all August measurements were from beech trees) prevents clear separation of seasonal and taxonomic effects.

Across all individuals, tree height (H) ranged from 26.4 to 35.3 m and showed a weak positive correspondence with primary and PSD peak frequencies (Table 1): trees with greater height (30.5–35.3 m) exhibited higher peak frequencies (0.23–0.26 Hz), while those with lower height (26.4–28.6 m) showed lower frequencies (0.18–0.20 Hz). Primary amplitudes (2,964–74,147) and total PSD values did not follow a consistent pattern with height. DBH ranged from 30.24 to 59.84 cm and showed a similar pattern: higher DBH values (39.15–59.84 cm) were generally associated with higher peak frequencies (0.23–0.25 Hz), but not with consistent changes in amplitude. The ratio DBH/H^2, calculated as a geometric proxy after Moore and Maguire (2004), ranged from 0.039 to 0.058 cm/m^2 and reflected the same frequency trend: lower ratios (0.039–0.044) corresponded to lower peak frequencies (0.20–0.23 Hz), while higher ratios (0.047–0.058) were associated with frequencies of 0.23–0.25 Hz. No consistent relationship was observed between DBH/H^2 and primary amplitudes or PSD power.

Singular value decomposition (SVD) applied to the spectrograms of individual sensor time series revealed consistent spatial and temporal patterns across co-located seismic sensors (Figure 6). The first three singular vectors accounted for approximately 40.8 % of the total variance in the spectrograms, with the leading mode alone explaining 23.9 %, indicating a strong low-rank structure even at the level of individual sensors. The temporal eigenvector amplitudes (panel A) show that dominant temporal modes (EV1–EV3) were expressed across all station types, with particularly strong and consistent contributions from the trunk-mounted accelerometers. In contrast, the spatial eigenvectors (panel B) highlight systematic differences in sensor sensitivity to each mode. Higher-mounted accelerometers tended to contribute more strongly to higher-order components, while the ground-based seismometer loaded more heavily on the first mode. These patterns suggest a vertical organization of sway dynamics, with spatial and temporal components separating vibrational modes by sensor position and complexity.

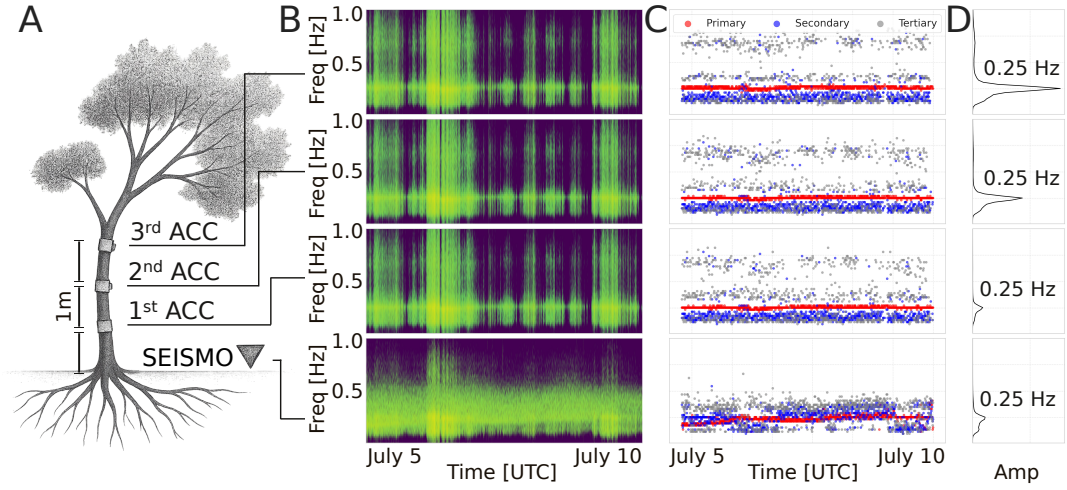

FIGURE 2 **A** The instrument set-up with three tree-attached accelerometers (ACC) and one co-located buried seismometer (SEISMO). **B** Spectrograms, **C** rolling spectral peaks using 10-minute moving windows applied to the Fourier-transformed signals, and **D** global amplitude spectra for the time period 07-05-2024 to 07-10-2024 of the pre-processed seismometer signal (*C67*) and accelerometer signals around tree *4_62* (Douglas fir, see Figure 1 for locations). All signals consistently exhibit a spectral peak near 0.25 Hz, with the amplitude increasing proportionally with sensor height. The primary peaks are shown in red, secondary in blue, and tertiary in grey.

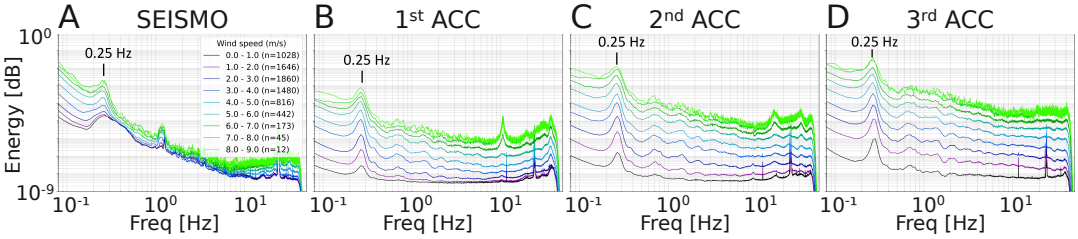

FIGURE 3 Wind-dependent Power Spectral Densities (PSDs) derived from **A** seismometer data and from **B–D** accelerometers mounted along the trunk of tree *4_62* (Douglas fir). PSDs are grouped and averaged by wind speed. *n* denotes the number of spectra averaged within each group, with fewer spectra available at higher wind speeds. To enable relative comparison between accelerometers, PSD amplitudes are commonly scaled. PSDs from all sensors exhibit a significant wind-dependent spectral peak at 0.25 Hz. An additional seismic peak at 1.15 Hz (**A**), which typically corresponds to the eigenfrequency of wind turbines, most likely originates from wind turbines located approximately 3 km away.

3.2 | Prediction of wind speed from seismic features

The XGBoost model was evaluated across a continuous period from July 2024 to March 2025 using a 5-fold block-wise cross-validation approach. The predicted wind speed closely followed the observed measurements (Figure 7A-B) and

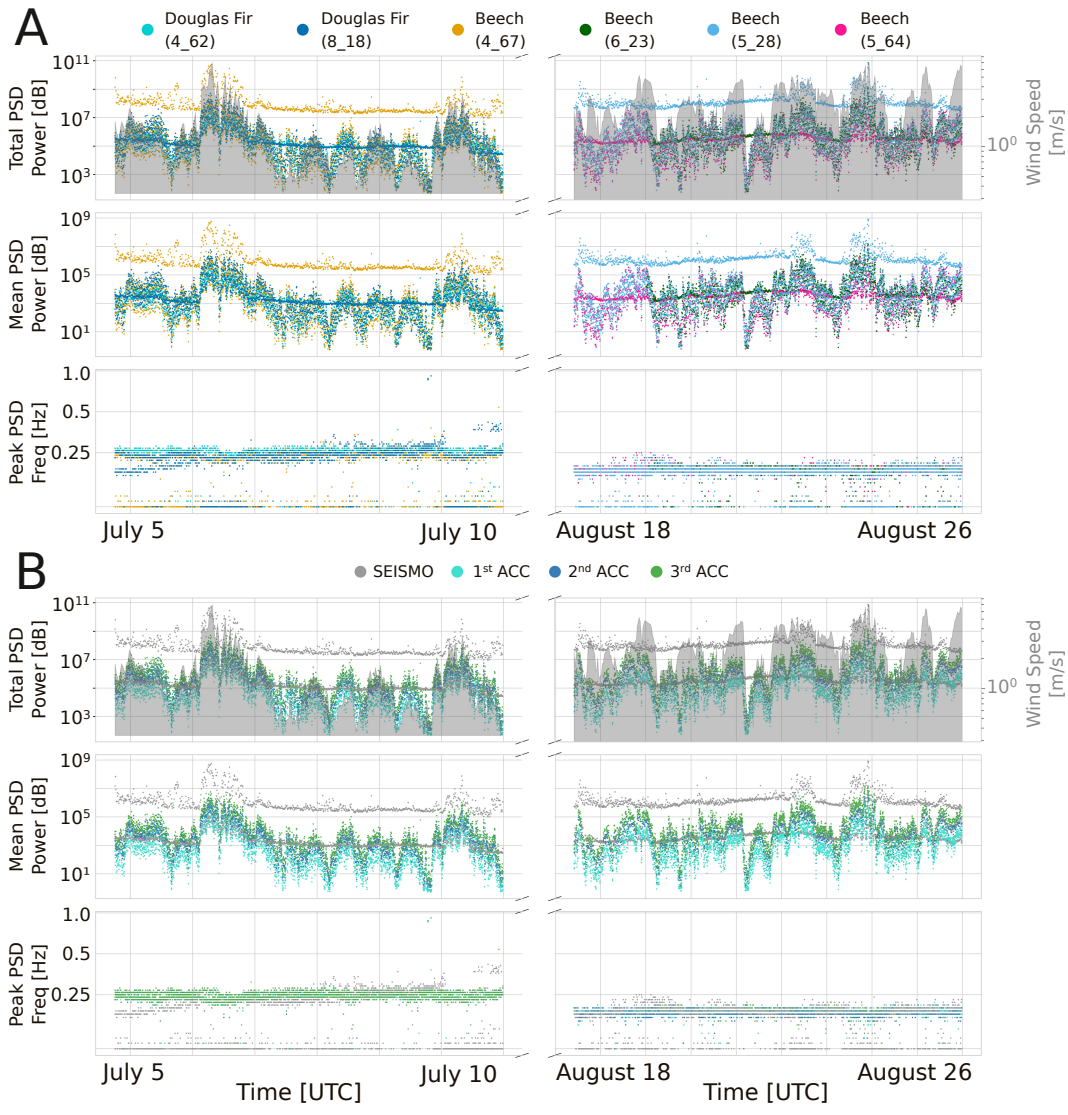

FIGURE 4 **A** Time-resolved PSD features (peak frequency, mean power, and total power) of all sensors (SEISMO, 1st ACC, 2nd ACC, 3rd ACC), color-coded by species. **B** Same peak data as in A, but color-coded by sensor type. Wind speed (in m/s) is shown as a filled grey area in the top subplot to indicate environmental forcing during the shared measurement periods (early July and late August 2024). All y-axes are log-scaled. Each point represents a PSD feature within a 10-minute time window.

no systematic overestimation or underestimations was detected (Figure 7C). The model achieved an RMSE of 1.092 (CC=0.80, MAPE=0.47) for training data and 1.088 (CC=0.79, MAPE=0.44) for test data. The SHAP feature attribution revealed varying importance of PSD frequencies, indicating that the total PSD power (22.20 %), peak PSD frequency

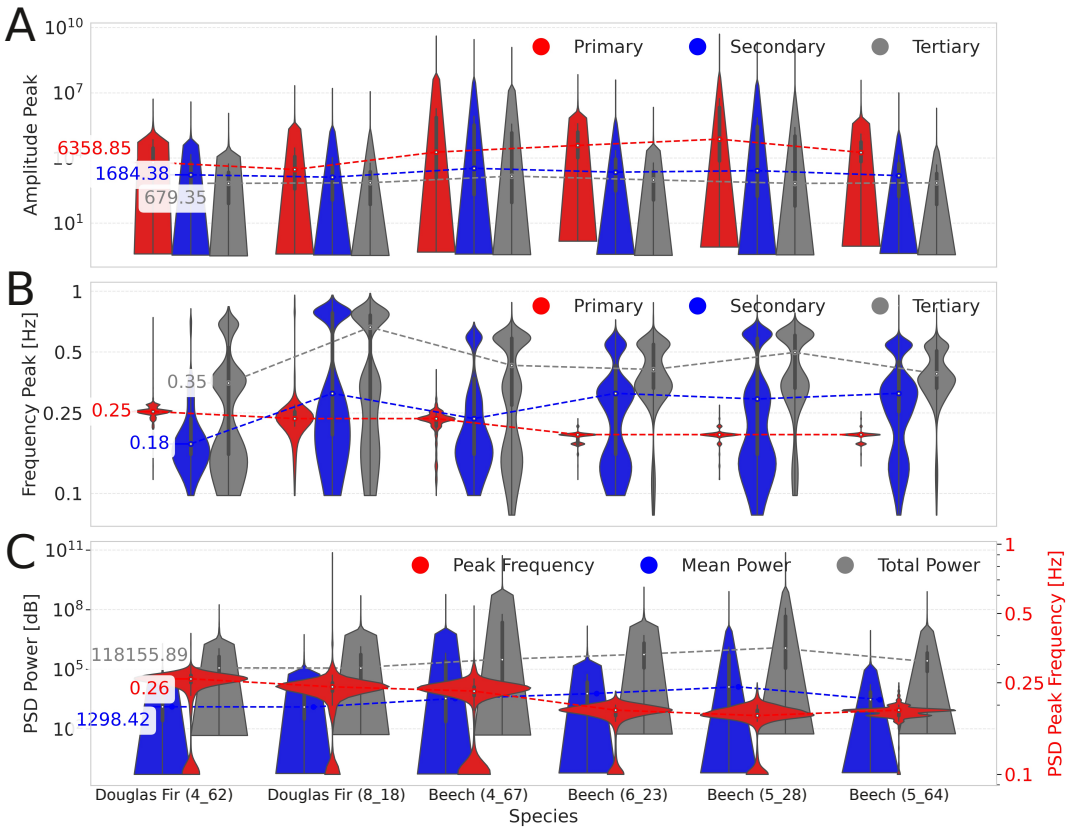

FIGURE 5 **A** Distribution of spectral peak amplitudes grouped by tree species. Individual tree IDs are given in brackets and link to Table 1. Peak types are color-coded as primary (red), secondary (blue), and tertiary (grey). **B** Corresponding violin plots of peak frequencies. **C** Distribution of PSD-based features by species: peak frequency (red), mean power (blue), and total power (gray). Red peak frequencies are plotted on a secondary y-axis. Dotted lines connect median values across species to illustrate relative shifts. All y-axes use a logarithmic scale.

(19.50 %), and secondary peak amplitude (19.50 %) contributed most prominently to the model's predictions (Figure 7D).

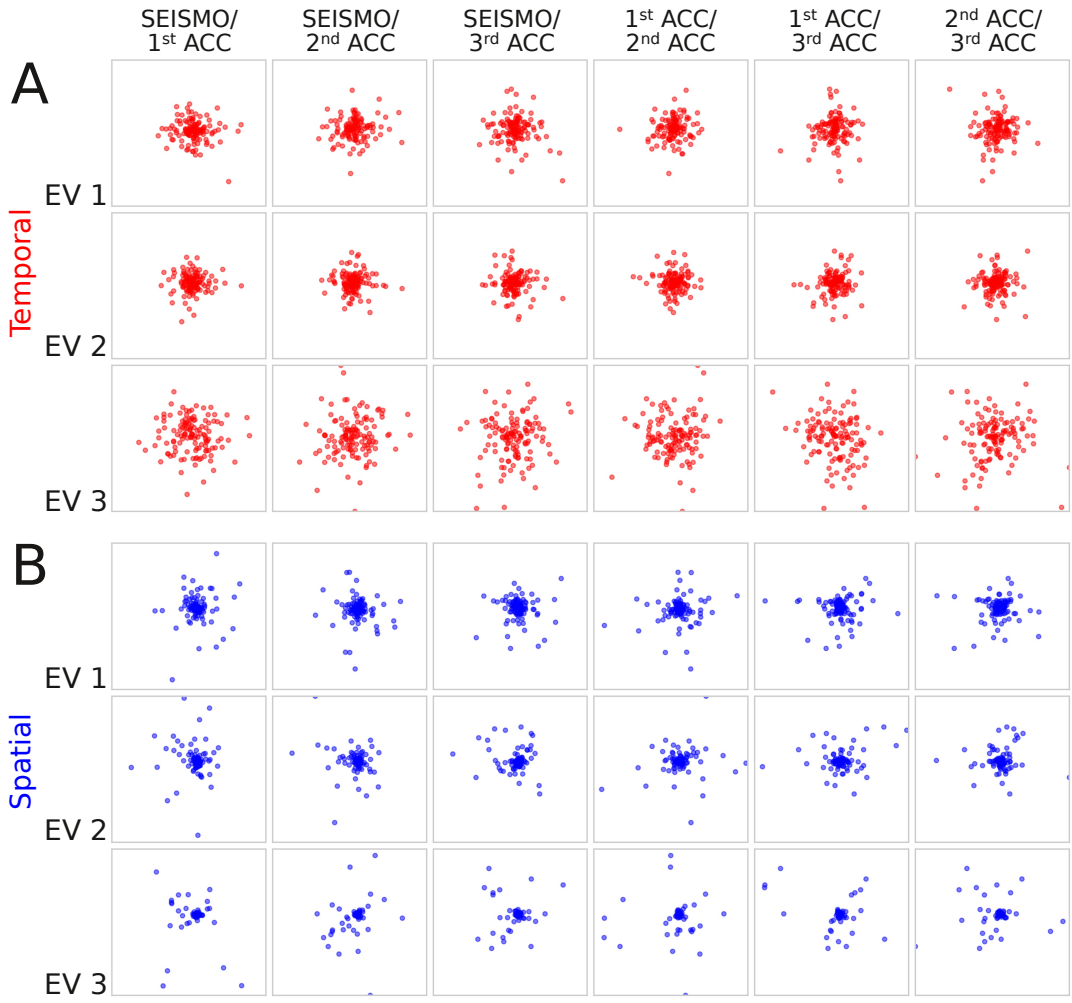

FIGURE 6 Singular value decomposition (SVD) results comparing temporal and spatial patterns across co-located sensors. **A** Temporal eigenvector amplitudes (red) for the first three components (EV1–EV3), shown for each station pair: the ground-based seismometer (SEISMO), and the first through third accelerometers (ACC) mounted on the same tree. **B** Spatial eigenvector amplitudes (blue) for the corresponding components and station pairs. Each triplet of bars reflects the relative contribution of that sensor to the respective mode, highlighting differences in temporal dynamics and spatial sensitivity across the seismic array. All eigenvector amplitudes are normalized, and consistent axis limits are applied across all panels to enable direct comparison. Tick positions are fixed at {-0.5, 0, 0.5} for spatial and {-0.02, 0, 0.02} for temporal components, based on the global minimum and maximum values across the entire dataset.

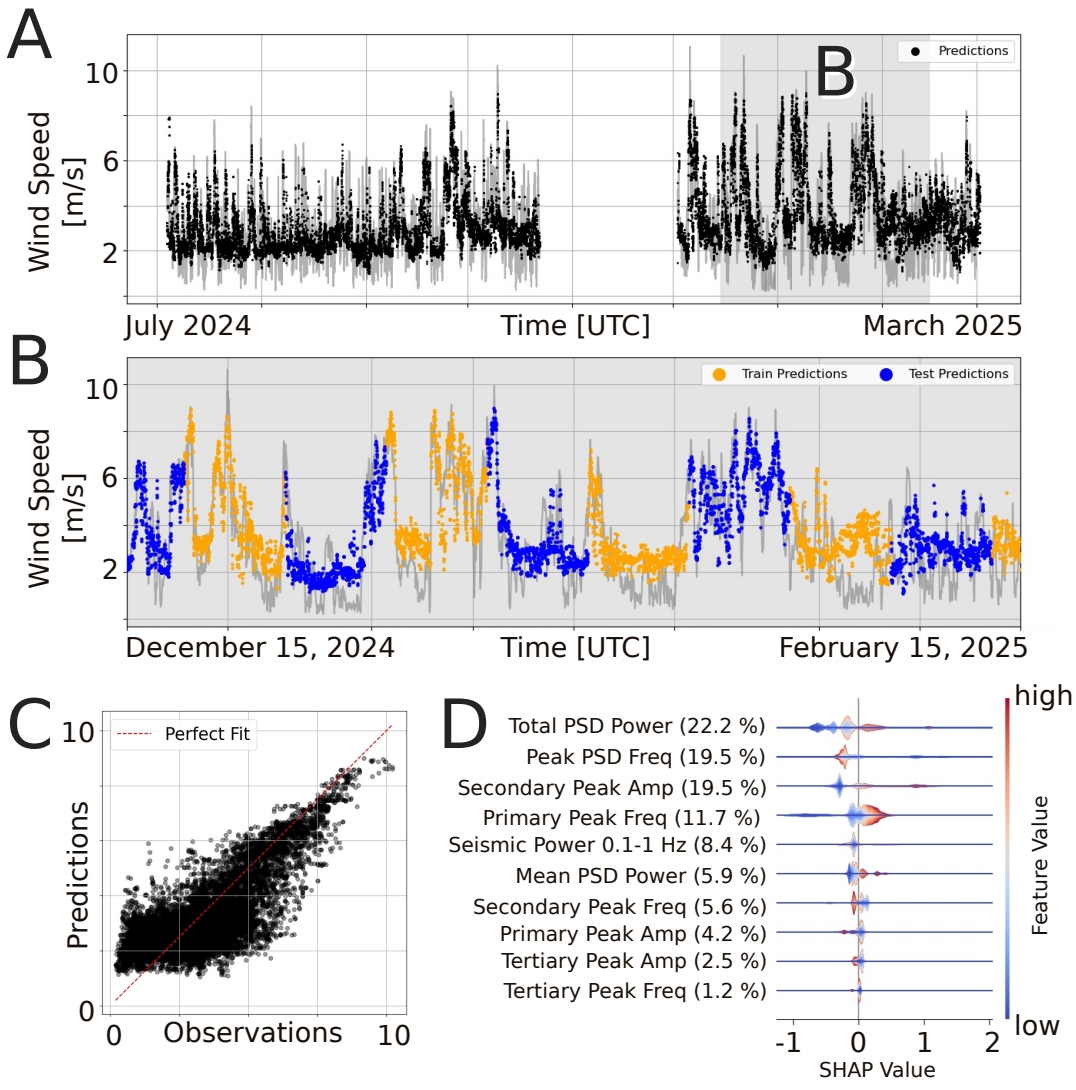

FIGURE 7 Predicting wind speed using only seismic features. **A** Wind speed observations (grey line) and model predictions (black scatterers) from July 2024 to March 2025 using a gradient-boosted tree model (XGB) with 5-fold cross-validation. A block-wise split with a window size of 7 days and a 1-hour rolling mean was applied. Training and test set performance reached an RMSE of 1.092 (CC=0.80, MAPE=0.47) and 1.088 (CC=0.79, MAPE 0.44), respectively. **B** Two-months zoom-in showing predictions by block, with orange scatterers indicating train performance and blue scatterers indicating test performance. **C** Predicted versus observed wind speed across all samples. **D** Feature importance based on mean absolute SHAP values (Lundberg and Lee, 2017), quantifying each feature's contribution to the model output.

4 | DISCUSSION

4.1 | Seismic monitoring as a scalable alternative to accelerometers

Our findings confirm that seismic measurements are a promising alternative to accelerometer-based monitoring of tree sway dynamics. By capturing the same dominant vibrational modes, particularly the fundamental sway frequency around 0.2 Hz, seismic sensors provide signals that are functionally equivalent to those obtained from accelerometers, but without requiring physical attachment to the tree. This fundamental frequency was consistently detected across species, environmental conditions, and over extended periods, demonstrating the robustness of the seismic approach. Importantly, seismic sway signals exhibited a clear and consistent dependence on wind forcing. The extracted spectral features, such as power, peak frequency, and amplitude, formed the basis of a predictive model that successfully inferred wind speed directly from ground motion. This confirms that seismic signals inherently encode the mechanical response of trees to wind, effectively capturing the input–output dynamics of tree sway. If wind forcing can be robustly inferred from seismic sway signatures, then the inverse problem - using changes in sway features as proxies for structural or physiological stress — becomes tractable. Such an approach could enable the detection of altered tree biomechanics under drought or other climate stressors, offering a scalable, non-invasive tool for forest health monitoring in a changing climate.

4.2 | Dominant sway frequency encodes tree structural properties

The stability and coherence of the dominant 0.25 Hz sway frequency across both trunk-mounted and ground-based sensors reflect a robust sway mode that spans the tree-stem–soil system. Its consistent presence across tree species, diameters, and heights, as well as under varying wind conditions, suggests it represents a fundamental structural property of the tree, rather than a transient or sensor-specific artifact. The vertical amplitude gradient observed along the trunk corresponds to a typical cantilever-like mode shape, with motion increasing toward the top. The detection of this resonance in seismometer recordings further confirms the strong coupling of aboveground tree sway into the

surrounding substrate. Notably, our analysis also showed that trees with greater height or higher DBH tended to sway at slightly higher fundamental frequencies, while the geometric ratio DBH/H^2, used as a proxy for mechanical stability, similarly tracked with changes in spectral content. These relationships reinforce the interpretation that sway frequency encodes structural information and that simple morphological metrics can meaningfully reflect a tree's dynamic response.

Our analysis of sway patterns using singular value decomposition (SVD) reveals that different parts of the tree respond differently to wind, and that these responses can be captured by both seismic and accelerometer sensors. Specifically, the strongest and most consistent sway signals, what we call the dominant vibration mode, were detected by all sensors over time. However, the sensor's location influenced what aspects of the sway it was most sensitive to. Accelerometers mounted higher on the trunk captured more complex, higher-order motion patterns, while the ground-based seismometer primarily detected the dominant, low-frequency sway of the entire tree. This confirms that tree sway is vertically structured (Kolbe et al., 2024), with distinct types of movement occurring at different heights. Here, we demonstrated that combining seismic and accelerometer data is essential to disentangle these layered dynamics. Ultimately, this spatial separation of vibrational modes offers a new way to study how trees sway from root to crown, opening the door to ecologically relevant insights into tree structure, stability, and wind exposure.

While the frequency content of primary and secondary spectral peaks remained relatively stable over time, these features consistently aligned with species-specific frequency bands. This spectral stability is consistent with structural resonances governed by tree architecture, such as height, diameter, and branching pattern. These resonance bands appeared in both accelerometer and seismic recordings, supporting their potential to characterize biomechanical traits across different trees. In contrast, tertiary peaks and PSD-derived peak frequencies exhibited greater temporal variability—especially in accelerometer data—suggesting they reflect more localized or flexible dynamics, such as branch motion or canopy flutter.

The temporal variation in secondary and tertiary peak occurrence likely reflects more localized or transient vibrational modes, possibly triggered by wind gusts, turbulence, or movement in finer branches (Kolbe et al., 2024). This interpretation is supported by the greater variability of these peaks in accelerometer data compared to seismic signals (Figure 2C and Supporting Figure S2), especially during periods of increased wind activity.

4.3 | Species-specific variation in sway dynamics

Species-specific clustering of peak frequencies and amplitudes (Figure 5) further suggests that differences in crown architecture, wood stiffness, and damping behaviour modulate these responses. Notably, higher-mounted accelerometers captured stronger and more frequent high-frequency components than lower-mounted ones or the seismometer (Figure 2D and Figure 6), indicating that sensor height plays a key role in resolving spectral detail. Additionally, broader distributions and lower amplitudes of tertiary peaks in some species may indicate greater structural flexibility or more complex modal behaviour. The drop-off in magnitude from primary to tertiary modes appears more pronounced in Douglas firs than in beeches, which may reflect interspecific differences in energy dissipation and biomechanical strategies to cope with wind exposure.

The species-specific differences in peak distributions, such as broader spreads and higher amplitudes in beech, likely stem from underlying biomechanical contrasts, including variations in stiffness, damping, and crown dynamics. That these differences persisted across trees of varying size suggests that structural architecture, rather than stem diameter alone, shapes the vibrational response. We confirmed that geometric scaling via DBH/H^2 offers a simple yet powerful way to compare trees of different sizes, revealing consistent trends with sway frequency. This supports long-standing theory that tree shape and structure influence how individuals respond to wind (Moore and Maguire, 2004). Trees with lower DBH/H^2 values swayed more slowly, reflecting more flexible or top-heavy forms, while those with higher ratios showed faster, stiffer motion. These differences suggest ecological significance: species with inherently higher DBH/H^2 ratios may be more wind-resilient, offering a biomechanically grounded trait for comparing species' vulnerability to storms and climate-driven mechanical stress.

Beyond static spectral characteristics, our time-resolved analysis revealed that wind acts as a dominant and dynamic modulator of tree sway signals. Periods of elevated wind speed consistently aligned with increases in spectral amplitude and total power, confirming that mechanical energy input from wind is reliably encoded in both accelerometer and seismic data. The strong temporal coherence observed across spectral peak amplitudes, dominant frequencies, and PSD power metrics indicates a robust physical coupling between environmental forcing and tree motion. These results reinforce the core premise of our approach: that seismic and accelerometer-based spectral features can serve

as scalable, passive proxies for real-time monitoring of wind-driven tree dynamics.

4.4 | Model limitations and seismic noise interference

While we demonstrate that seismometers are capable of capturing characteristic vibrational components of a nearby tree, other noise sources, such as wind turbines in the vicinity, may be mistakenly interpreted as tree-induced ground motion, as shown by the significant 1.15 Hz peak identified in Figure 3. Both trees and wind turbines exhibit similar vibrational behaviour, with eigenfrequencies excited by wind forcing either the tree canopy or the turbine tower due to the turbines rotation. Wind turbines typically emit signals predominantly above 1 Hz detectable kilometres away (Zieger and Ritter, 2018; Neuffer and Kremers, 2017), with distinct frequency peaks consistently observable at all seismometers in the vicinity. Hence, they share a common frequency range as trees (0.1–5 Hz), depending on the dimensions and properties of the trees. Another notable parallel between trees and wind turbines are potential interferences of wave fields emitted by multiple resonators of its kind (forest or wind farms) which, on the one hand, complicates a robust detection and characterization of the wind-dependent and dynamic wave fields. On the other hand, this allows the detection of multiple seismic fingerprints simultaneously (Limberger et al., 2021). As shown with our dataset, different types of trees in a forest contribute in distinct ways to the complex, superimposed wave field recorded by one or more seismometers in a forest. This highlights the importance of identifying and constraining the primary contributing features and spatial dependencies.

Additionally, ocean microseismic noise falls within a similar frequency range as the fundamental tree sway frequency (Hasselmann, 1963). In particular, during winter months when ocean conditions are rougher, this background noise can mask tree vibrations. In contrast, such noise levels are significantly lower in the summer, improving the chances of detecting tree-induced signals as demonstrated in our study.

Nonetheless, model limitations were evident at the boundaries of the wind speed distribution. Under low wind conditions (below 2 m/s), the model tended to over-predict, while short-lived high wind peaks were occasionally underestimated. These discrepancies likely stem from the temporal smoothing of features and the limited responsiveness of some input variables to rapid changes. Also, the seismic sensors may not be sensitive to slight vibrational changes at

low wind speeds (approximately between 0–2 m/s, Figure 3A), as dominant external seismic noise sources can reduce their sensitivity. In contrast, accelerometers provide sensitivity during low wind speeds (Figure 3B–D), when attached to the stem allowing robust detection of small vibrational changes. Feature importance analysis using SHAP values revealed that total PSD power, peak PSD frequency, and secondary peak amplitude were the most influential predictors. Notably, broadband PSD metrics outperformed many peak-based features, suggesting that aggregate spectral energy more robustly encodes wind forcing (Spatz and Theckes, 2013). Still, higher-order peak amplitudes and frequencies contributed additional predictive value, indicating that fine spectral structure plays a supporting role. These findings underscore the utility of passive seismic features for estimating wind conditions but also point toward opportunities to improve prediction accuracy, particularly under extreme or rapidly fluctuating environmental scenarios.

5 | CONCLUSIONS

This study demonstrates that seismic measurements can serve as a viable, scalable alternative to accelerometer-based methods to capture wind-induced tree sway. By isolating species-specific vibrational signatures in both seismic and acceleration data, we show that fundamental sway modes, particularly around 0.2 Hz, are consistently detectable across species, stem diameters, heights, and environmental conditions. These low-frequency resonance patterns reflect a robust mechanical response of trees and highlight the potential for seismometers to passively monitor biomechanical behaviour without direct attachment to individual trees.

Our frequency-based analyses reveal a structured and vertically differentiated sway response. Accelerometers mounted higher on trunks captured more complex, high-frequency motion patterns, while ground-based seismometers were most sensitive to the dominant stem-level sway. This vertical organisation of sway dynamics underscores the value of combining both sensor types to resolve layered movement patterns from root to crown.

Importantly, we found that structural traits such as tree height, DBH, and the geometric ratio DBH/H^2 correlated with sway frequency. While mathematical theory already tells us that morphological metrics can predict how trees respond to wind, our results demonstrate that these relationships can be observed passively through seismic

measurements. Trees with greater height or higher DBH exhibited slightly elevated peak frequencies, while those with lower DBH/H² ratios swayed more slowly, consistent with more top-heavy or flexible forms. This novel insight strengthens the interpretation of seismic sway signals as expressions of underlying biomechanics, offering a pathway toward linking vibrational signatures to physical structure in a non-invasive and scalable way.

Critically, spectral features extracted from seismic data enabled accurate prediction of wind speeds using machine learning, confirming that wind-induced sway is reliably encoded in ground motion. This supports the core premise of our study: that seismic signals inherit meaningful biomechanical information and can serve as proxies for environmental forcing. Looking ahead, this approach offers a way to monitor tree condition over time - where deviations in sway behaviour could signal changes in structural integrity, water status, or vulnerability to storm damage.

As climate change increases the frequency and severity of both drought and mechanical disturbance, there is growing need for low-maintenance, scalable methods to assess tree health and stability. Our findings suggest that the seismic fingerprint of tree sway is not merely a side effect of motion, but a valuable ecological signal. With further development, this method could support long-term forest monitoring and early warning systems grounded in the principles of environmental seismology. Compared to accelerometers, seismometers offer a less invasive, more scalable solution, which is well-suited for continuous, multi-tree monitoring across forest plots. By capturing both vitality-related changes (e.g., reduced damping under drought) and indicators of structural vulnerability (e.g., resonance shifts before failure), seismic sway sensing offers a unified framework for tracking forest resilience under climate extremes.

AUTHOR CONTRIBUTIONS

J. Umlauft, K. Gerberding, and T. Kattenborn acquired the seismic and acceleration data in the field. C. Werner provided the wind speed data. J. Umlauft performed the data analysis, including preprocessing, frequency analysis, eigenvalue analysis, correlation analysis, and machine learning. F. Limberger performed the PSD analysis. The study was conceptualized by J. Umlauft, T. Kattenborn, and K. Mora. The manuscript was written by J. Umlauft. All other coauthors discussed and contributed critically to the drafts and gave final approval for publication.

ACKNOWLEDGMENTS

The authors gratefully acknowledge financial support from the Federal Ministry of Research, Technology and Space of Germany, as well as from the Saxon State Ministry for Science, Culture and Tourism through the Center of Excellence for AI Research "Center for Scalable Data Analytics and Artificial Intelligence Dresden/Leipzig" (ScaDS.AI), project identification number: ScaDS.AI. We also acknowledge funding from the DFG-funded Collaborative Research Centre CRC-1537 ECOSENSE. We thank Maximilian Fabi and Daniel Lusk for their assistance during fieldwork, and Geophysical Instrument Pool Potsdam (GIPP) - especially Dr. Christian Haberland - for consultation and providing instrumentation. Finally, we are grateful to the iDiv Research Platform ARBOfun – Research Arboretum Großpösna for supporting preliminary tests and contributing to the conceptual development of the study in course of the CRC proposal BBCe (Biodiversity Buffers Climate Extremes).

DATA AVAILABILITY STATEMENT

Data and code will be made publicly available upon acceptance. Specifically, we will use the platforms Github Digital Repository (https://github.com/) and Zenodo (https://zenodo.org/), for which a doi will be assigned and reported in the paper. Furthermore the full data citation will then be given in the reference list.

CONFLICT OF INTEREST

The authors declare no conflict of interest.

REFERENCES

Allen, C. D., Breshears, D. D. and McDowell, N. G. (2015) On underestimation of global vulnerability to tree mortality and forest die-off from hotter drought in the anthropocene. *Ecosphere*, **6**, 1–55.

Brüchert, F., Speck, O. and Spatz, H.-C. (2003) Oscillations of plants' stems and their damping: theory and experimentation. *Philosophical Transactions of the Royal Society of London. Series B: Biological Sciences*, **358**, 1487–1492.

Chen, T. and Guestrin, C. (2016) Xgboost: A scalable tree boosting system. In *Proceedings of the 22nd ACM SIGKDD International Conference on Knowledge Discovery and Data Mining*, KDD '16, 785–794. New York, NY, USA: Association for Computing Machinery. URL: https://doi.org/10.1145/2939672.2939785.

Ciruzzi, D. M. and Loheide II, S. P. (2019) Monitoring tree sway as an indicator of water stress. *Geophysical Research Letters*, **46**, 12021–12029. URL: https://agupubs.onlinelibrary.wiley.com/doi/abs/10.1029/2019GL084122.

— (2021) Monitoring tree sway as an indicator of interception dynamics before, during, and following a storm. *Geophysical Research Letters*, **48**, e2021GL094980.

Colombi, A., Roux, P., Guenneau, S. et al. (2016) Forests as a natural seismic metamaterial: Rayleigh wave bandgaps induced by local resonances. *Scientific Reports*, **6**, 19238. URL: https://doi.org/10.1038/srep19238.

van Emmerik, T., SteeleDunne, S., Hut, R., Gentine, P., Guerin, M., Oliveira, R. S., Wagner, J., Selker, J. and van de Giesen, N. (2017) Measuring tree properties and responses using low-cost accelerometers. *Sensors*, **17**, 1098.

Gassner, L. and Ritter, J. (2023) Ground motion emissions due to wind turbines: observations, acoustic coupling, and attenuation relationships. *Solid Earth*, **14**, 785–803.

Ghonimy, M., Alharbi, A. and Ibrahim, M. M. (2025) Damping behavior of olive trees under trunk shaking. *Scientific Reports*, **15**.

Giachetti, T., Bonnesoeur, V., Jay-Allemand, M., Barbacci, A. and Van Esperen, E. (2022) A low-cost accelerometer-based system for in-situ monitoring of tree sway: linking mechanical traits to water status. *Forests*, **13**, 1243.

Grande, E., Giordano, E. and Clementi, F. (2023) Evaluation of dynamic properties of trees subjected to induced vibrations. *Applied Sciences*, **13**, 7333.

Hasselmann, K. (1963) A statistical analysis of the generation of microseisms. *Reviews of Geophysics*, **1**, 177–210.

Jackson, B., Kohler, M., Moore, J. R., Spatz, H.-C. and Speck, T. (2019) Mechanics explains deviations from leaf economic spectrum: evidence from leaf mass, venation and biomechanics across australian species. *Journal of The Royal Society Interface*, **16**, 20190116.

Jackson, T. D., Sethi, S., Dellwik, E., Angelou, N., Bunce, A., van Emmerik, T., Duperat, M., Ruel, J.-C., Wellpott, A., Van Bloem, S., Achim, A., Kane, B., Ciruzzi, D. M., Loheide II, S. P., James, K., Burcham, D., Moore, J., Schindler, D., Kolbe, S., Wiegmann, K., Rudnicki, M., Lieffers, V. J., Selker, J., Gougherty, A. V., Newson, T., Koeser, A., Miesbauer, J., Samelson, R., Wagner, J., Ambrose, A. R., Detter, A., Rust, S., Coomes, D. and Gardiner, B. (2021) The motion of trees in the wind: a data synthesis. *Biogeosciences*, **18**, 4059–4072. URL: https://bg.copernicus.org/articles/18/4059/2021/.

Johnson, C. W., Meng, H., Vernon, F. and Ben-Zion, Y. (2019) Characteristics of ground motion generated by wind interaction with trees, structures, and other surface obstacles. *Journal of Geophysical Research: Solid Earth*, **124**.

Kolbe, S., Kammel, F., Schmitt, A., Reiterer, A. and Schindler, D. (2024) Mode coupling and signal energy distribution in an open-grown european beech tree. *Forest Ecology and Management*, **560**, 121845. URL: https://www.sciencedirect.com/science/article/pii/S0378112724001579.

Larose, E., Carrière, S., Voisin, C., Bottelin, P., Baillet, L., Guéguen, P., Walter, F., Jongmans, D., Guillier, B., Garambois, S., Gimbert, F. and Massey, C. (2015) Environmental seismology: What can we learn on earth surface processes with ambient noise? *Journal of Applied Geophysics*, **116**, 62–74.

Limberger, F., Lindenfeld, M., Deckert, H. and Rümpker, G. (2021) Seismic radiation from wind turbines: observations and analytical modeling of frequency-dependent amplitude decays. *Solid Earth*, **12**, 1851–1864.

Liu, Y., Huang, J., Li, Y. and Shi, Z. (2019) Trees as large-scale natural metamaterials for low-frequency vibration reduction. *Construction and Building Materials*, **199**, 737–745. URL: https://www.sciencedirect.com/science/article/pii/S0950061818330459.

Lundberg, S. M. and Lee, S.-I. (2017) A unified approach to interpreting model predictions. In *Advances in Neural Information Processing Systems*, vol. 30, 4765–4774. Curran Associates, Inc.

Moore, J. R. and Maguire, D. A. (2004) Natural sway frequencies and damping ratios of trees: concepts, review and synthesis of previous studies. *Trees*, **18**, 195–203.

Neuffer, T. and Kremers, S. (2017) How wind turbines affect the performance of seismic monitoring stations and networks. *Geophysical Journal International*, **211**, 1319–1327. URL: https://doi.org/10.1093/gji/ggx370.

Raleigh, M., Verhoest, N. and Dale, J. (2022) Challenges and capabilities in estimating snow mass intercepted in conifer canopies with tree sway monitoring. *Water Resources Research*, **58**, e2021WR030972. URL: https://agupubs.onlinelibrary.wiley.com/doi/10.1029/2021WR030972.

Shearer, P. M. (2009) *Introduction to Seismology*. Cambridge, UK: Cambridge University Press, second edn.

Spatz, H.-C. and Theckes, B. (2013) Oscillation damping in trees. *Plant Science*, **207**, 66–71. URL: https://www.sciencedirect.com/science/article/pii/S0168945213000460.

Wang, Y., Xu, L., Zhang, Y., Zhu, Y., Zhou, H., Cui, W. and Zhang, A. (2024) Study of vibration patterns and response transfer relationships in walnut tree trunks. *Scientia Horticulturae*, **337**, 113567.

Welch, P. (1967) The use of fast fourier transform for the estimation of power spectra: A method based on time averaging over short, modified periodograms. *IEEE Transactions on Audio and Electroacoustics*, **15**, 70–73.

Werner, C., Bahn, M., Grams, T. E. E., Grossiord, C., Haberstroh, S., Lenczner, G., Tuia, D. and Vallicrosa, H. (2025) Impact of emerging compound droughts on forests: a water supply and demand perspective. *Plant Biology*.

Werner, C., Wallrabe, U., Christen, A., Comella, L., Dormann, C., Göritz, A., Grote, R., Haberstroh, S., Jouda, M., Kiese, R. et al. (2024) Ecosense-multi-scale quantification and modelling of spatio-temporal dynamics of ecosystem processes by smart autonomous sensor networks. *Research Ideas and Outcomes*, **10**, e129357.

Zieger, T. and Ritter, J. (2018) Influence of wind turbines on seismic stations in the upper rhine graben, sw germany. *Journal of Seismology*, **22**.

Supporting Information for:

The Seismic Fingerprint of Tree Sway

Josefine Umlauft[1] | Karin Mora[2] | Fabian Limberger[3] | Kilian Gerberding[4] | Christian Wirth[5] | Christiane Werner[6] | Teja Kattenborn[4]

[1]ScaDS.AI – Center for Scalable Data Analytics and Artificial Intelligence, Leipzig University

[2]Institute for Earth System Science & Remote Sensing, Leipzig University

[3]Goethe University Frankfurt am Main

[4]Sensor-based Geoinformatics, University of Freiburg

[5]Institute of Systematic Botany and Functional Biodiversity, Leipzig University

[6]Ecosystem Physiology, University of Freiburg

CONTENTS

REFERENCES

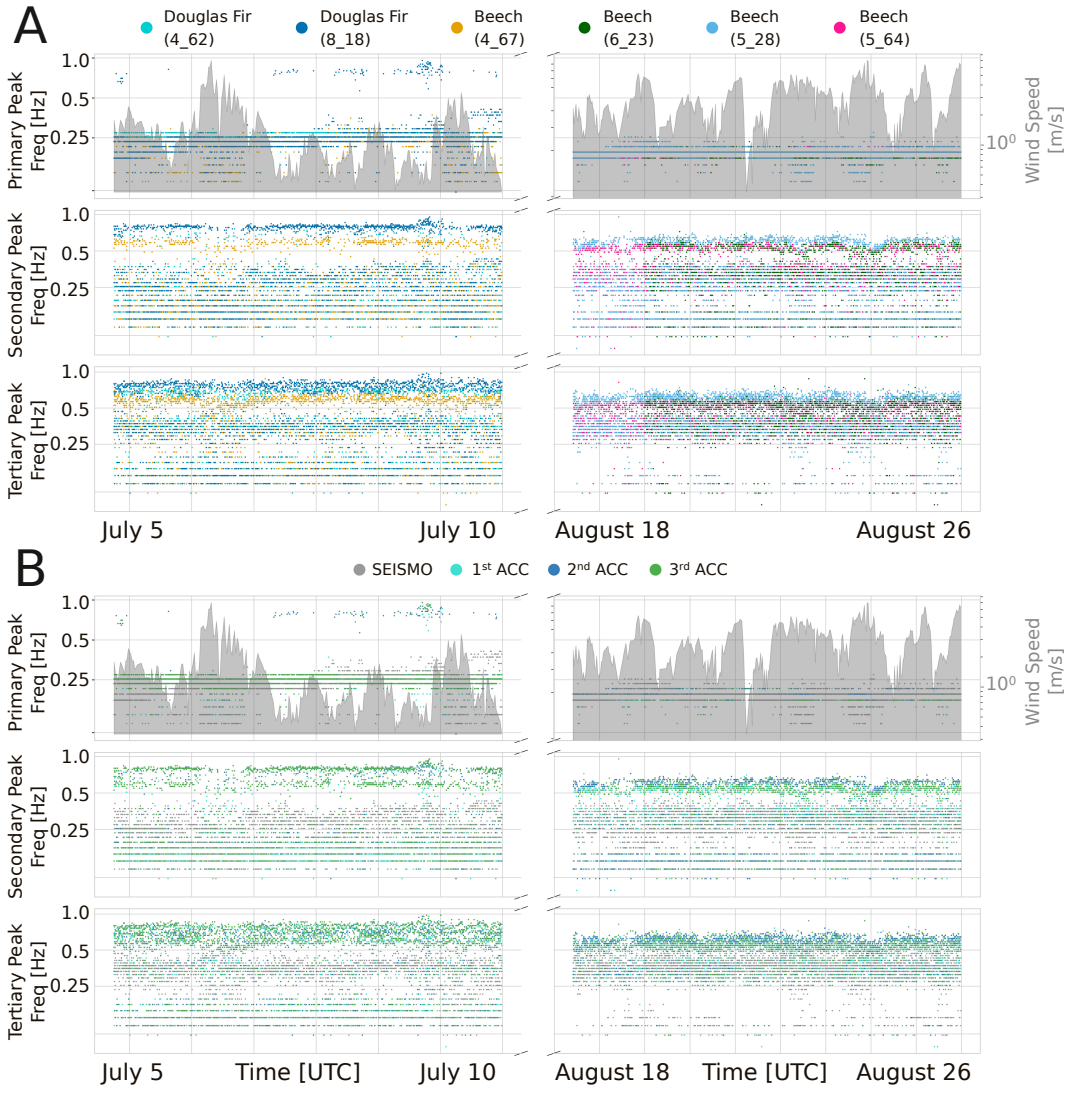

FIGURE S1 **A** Time-resolved spectral peaks (primary, secondary, and tertiary) of all sensors (SEISMO, 1st ACC, 2nd ACC, 3rd ACC), color-coded by species. **B** Same peak data as in A, but color-coded by sensor type. Wind speed (in m/s) is shown as a filled grey area in the top subplot to indicate environmental forcing during the shared measurement periods (early July and late August 2024). All y-axes are log-scaled. Each point represents a detected peak frequency within a 10-minute time window.

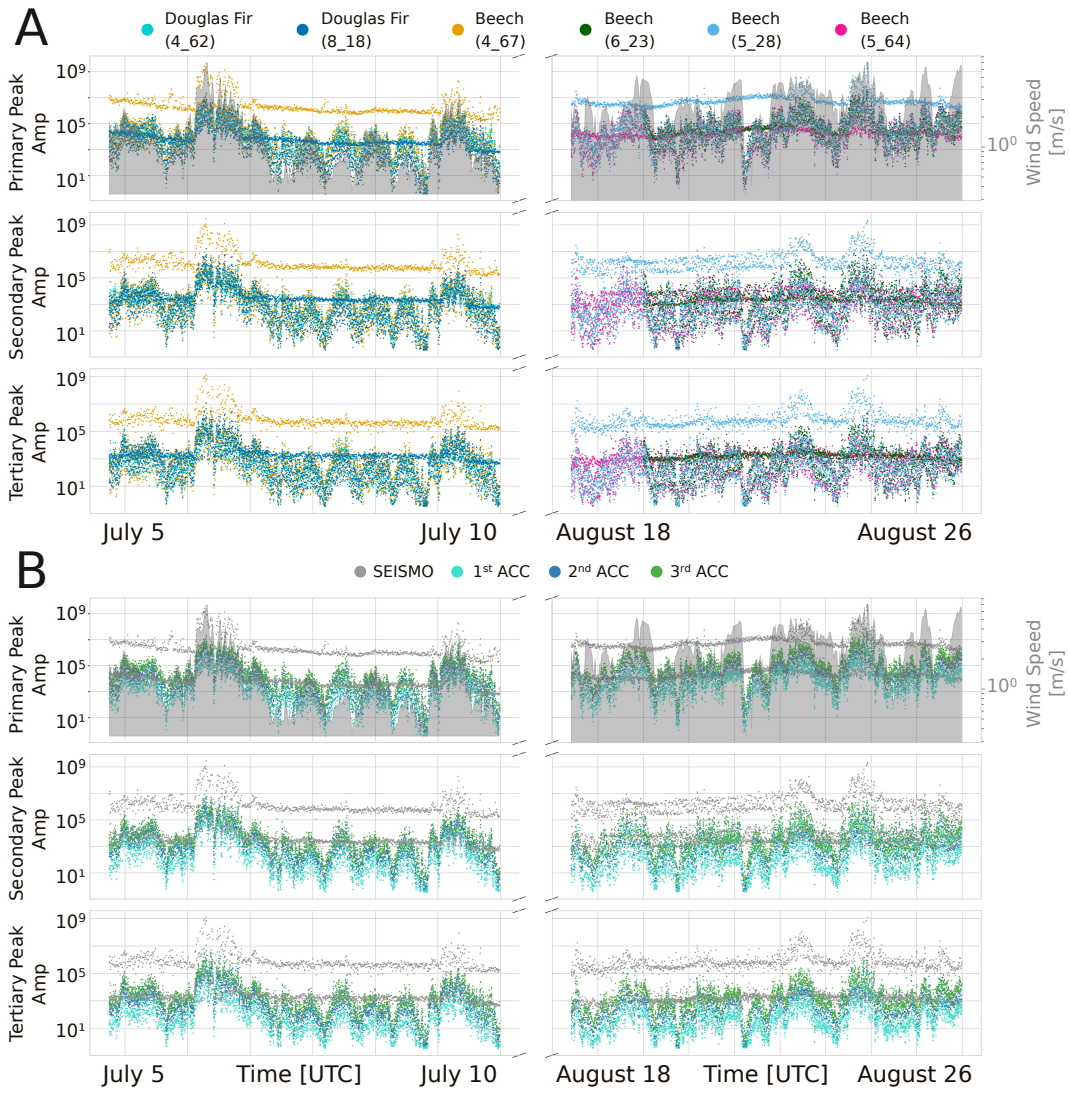

FIGURE S2 **A** Time-resolved spectral peak amplitudes (primary, secondary, and tertiary) of all sensors (SEISMO, 1st ACC, 2nd ACC, 3rd ACC), color-coded by species. **B** Same peak data as in A, but color-coded by sensor type. Wind speed (in m/s) is shown as a filled grey area in the top subplot to indicate environmental forcing during the shared measurement periods (early July and late August 2024). All y-axes are log-scaled. Each point represents a detected peak amplitude within a 10-minute time window.

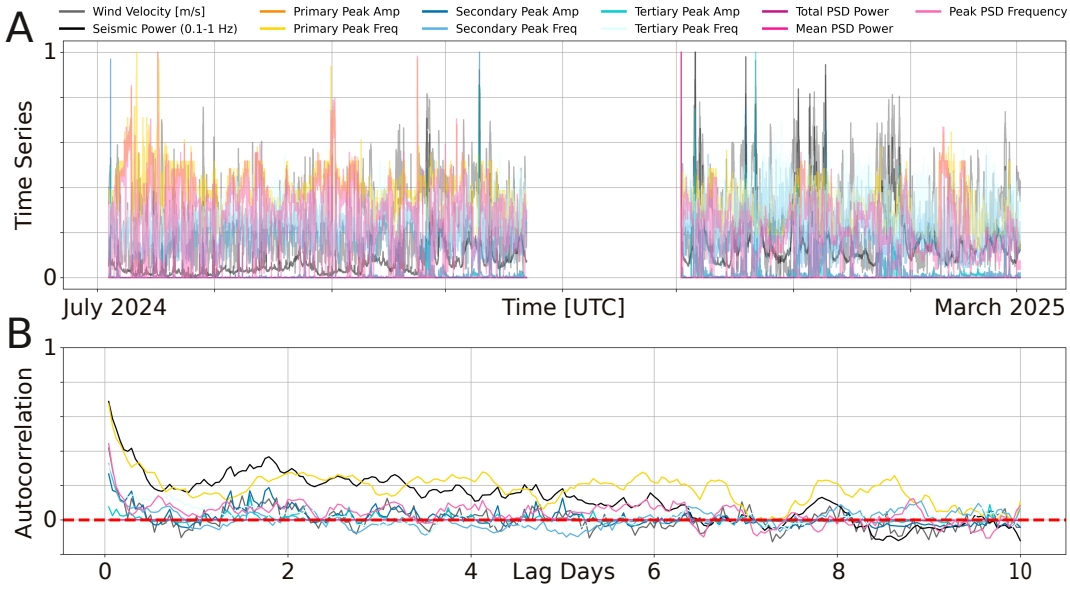

FIGURE S3 **A** Normalized time series of all model input features and the target variable (wind velocity). **B** Corresponding autocorrelation functions of the same features and target. Each time series represents the median value across all seismometers, computed at 1-minute intervals. Features include seismic power in the 0.1–1 Hz band, as well as primary, secondary, and tertiary peak frequencies and their corresponding amplitudes, all extracted from spectrograms. Further, summary features were derived from PSD analysis which include total PSD power, mean PSD power, and peak PSD frequencies. Prior to modeling, the time series were smoothed using a rolling mean to reduce high-frequency noise.